ELSEVIER

www.elsevier.nl/locate/jorganchem

Journal of Organometallic Chemistry 598 (2000) 248–253

Journal of Organometallic Chemistry

Synthesis, structure and coordination chemistry of mono- and bis-heterocyclic-ferrocenyl derivatives

Christian J. Isaac [a], Clayton Price [a], Benjamin R. Horrocks [a], Andrew Houlton [a,*], Mark R.J. Elsegood [b], William Clegg [b]

[a] *Department of Chemistry University of Newcastle upon Tyne, Newcastle upon Tyne NE1 7RU, UK*
[b] *Department of Chemistry, Crystallography Laboratory, University of Newcastle upon Tyne, Newcastle upon Tyne NE1 7RU, UK*

Received 31 July 1999; received in revised form 21 November 1999

Abstract

The heterocyclic-ferrocenyl derivatives, 1,1′-bis(5-phenanthridine)ferrocene (**1**) and [Pd{(η^5-C_5H_5)Fe(η^5-C_5H_3(phenanthroline))}Cl] (**2**), have been prepared and characterised by single-crystal X-ray analyses. These confirm that in **1** the substitution at the heterocycle is *ortho* to the nitrogen atom of the phenanthridine while for **2** *ortho*-metallation of the ferrocenyl group is observed in addition to chelation of the Pd(II) by the phenanthroline moiety. © 2000 Elsevier Science S.A. All rights reserved.

Keywords: Ferrocenyl; Heterocyclic; Palladium

1. Introduction

The attachment of aromatic heterocycles, such as bipyridyl or phenanthroline, to the ferrocenyl group has been one strategy for locating a metal binding site in close proximity to a redox-active moiety [1–3]. Complexation reactions with Pd [2] and Ru [2] have been reported for such derivatives with binding involving the nitrogen donor atoms, though additional binding can also occur, particularly in the former case, through cyclometallation. Such reactions have often been reported for dimethylaminomethyl-substituted ferrocenyl derivatives [4].

Alternative applications for heterocyclic-ferrocenyl derivatives include the design of redox-active compounds for probing DNA structure and uses for compounds that exhibit either covalent or non-covalent binding have been described [5–7]. We are interested in the synthesis of such compounds and here report the preparation, electrochemical behaviour and the molecular and crystal structure of a novel bis-substituted derivative 1,1′-bis(5-phenanthridine)ferrocene and also a ferrocenyl analogue, [Pd{($\eta^5C_5H_5$)Fe($\eta^5C_5H_3$-($C_{12}H_7N_2$))}Cl], of the DNA-nicking palladium complexes of general type [PdCl(2-phenyl-1,10-phenanthroline)] [8,9].

2. Results and discussion

2.1. Syntheses

1,1′-Bis(5-phenanthridine)ferrocene was prepared by the method reported by Butler for 2-ferrocenyl-1,10-phenanthroline and other heterocyclic derivatives [1,2]. This involves the initial formation of a suspension of mono/dilithioferrocene, generated by reaction of ferrocene with *n*-butyllithium, with subsequent addition of the appropriate heterocycle under N_2. Subsequent work up is in air to achieve oxidation of the expected dihydro intermediates [10], after which the crude mixture is then separated by column chromatography on silica to afford the pure product(s) [1,2].

The reaction yielded a mixture of ferrocene and unreacted phenanthridine along with three additional products as determined by TLC. Compared with the cases of 1,10-phenanthroline and bipyridyls [1,2], the reaction with phenanthridine gave a poorer overall yield and the major product was the bis-substituted

* Corresponding author. Fax: +44-191-222-6929.
E-mail address: andrew.houlton@ncl.ac.uk (A. Houlton)

PII: S0022-328X(99)00717-2

derivative (mono/bis product ratio ~1:5). The amount of unreacted starting materials obtained is significant, with ~40% ferrocene being recovered. In view of the crystal structure analysis (vide infra), it is suggested that the low yield is due to steric hindrance resulting from the site of attachment of the ferrocenyl group to the phenanthridine moiety. This is also in keeping with the difficulties in attempted alkylation reactions.

To our knowledge, no ferrocenylphenanthridine derivatives have been previously reported; however, the site of substitution at the phenanthidine is *ortho* to the nitrogen atom as expected. This was confirmed unequivocally by a single-crystal X-ray analysis.

2.2. Crystal structure of 1,1′-bis(5-phenanthridine)ferrocene (1)

Single crystals of 1,1′-bis(5-phenanthridine)ferrocene suitable for X-ray crystallography were obtained by slow evaporation of a solution in hexanes–ether (1:1). The molecular structure is shown in Fig. 1, which also indicates the crystallographic atomic numbering scheme. Selected molecular geometry parameters are presented in Table 1.

The Cp rings of the ferrocenyl group are approximately eclipsed (7.0° twist about the line joining the ring centroids) with an interplanar angle of 1.7° (Fig. 2). The phenanthridine substituents are bonded to the Cp rings through the C5 position of the heterocycles in each case (C(13) and C(24) according to the molecular numbering scheme), as expected from related chemistry [1,2,10], and are essentially in a *cisoid*-configuration. The variations in the Fe–C bond lengths are small, 2.0389(16)–2.0670(15) Å (mean 2.0524 Å), with the longer distances involving the two carbons bearing the substituent phenanthridine groups (C(14) and C(23)). The effects of these substituents on the geometry of the Cp rings are also apparent in the ring C–C distances and C–C–C angles and similar effects have been noted for 1,1′-bis(anthracenyl)ferrocene [11]. The iron-ring centroid distances are 1.658 Å for the Cp-containing C(14)–C(18) and 1.652 Å to the Cp-containing C(19)–C(23). Comparisons with other disubstituted ferrocenyl derivatives found in the Cambridge Structural Database show these distances to be unexceptional [12].

Table 1
Selected bond lengths (Å) for 1,1′-bis(5-phenanthridine)ferrocene (1)

Fe–C(14)	2.0670(15)	Fe–C(23)	2.0617(16)
Fe–C(15)	2.0637(17)	Fe–C(22)	2.0539(16)
Fe–C(16)	2.0523(17)	Fe–C(21)	2.0513(17)
Fe–C(17)	2.0457(17)	Fe–C(20)	2.0450(16)
Fe–C(18)	2.0448(16)	Fe–C(19)	2.0389(16)
C(14)–C(18)	1.436(2)	C(14)–C(15)	1.434(2)
C(15)–C(16)	1.415(2)	C(16)–C(17)	1.421(3)
C(17)–C(18)	1.424(2)	C(23)–C(22)	1.435(2)
C(23)–C(19)	1.433(2)	C(19)–C(20)	1.420(2)
C(20)–C(21)	1.423(3)	C(21)–C(22)	1.423(2)

The bond lengths and angles associated with the phenanthridine rings show little deviation from those of the free phenanthridine [13]. The phenanthridine units are not co-planar with the parent Cp rings as indicated by the interplanar angles between the respective Cp rings and phenanthridine moieties (30.1° Cp–N(1) and 31.6° Cp–N(2)). The two-phenanthridine substituents are inclined at an angle of 9.9° with respect to each other. The molecular structure in Fig. 2 shows the view looking down the Cp–Fe–Cp axis and clearly illustrates that the two phenanthridine units are eclipsed in the solid state. Again, this is similar to the structure of the related disubstituted derivative, 1,1′-bis(anthracenyl)ferrocene [11]. On steric grounds a 180° rotation of one of the Cp rings to the *transoid* conformation may be expected; however, the interligand π–π stacking could account for the observed eclipsing of the phenanthridine ligands (mean separation between the two phenanthridine substituent groups ca 3.5 Å). The crys-

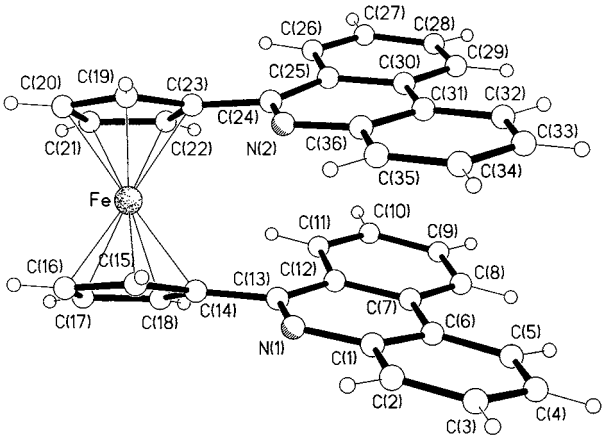

Fig. 1. Molecular structure of 1,1′-bis(5-phenanthridine)ferrocene (1), showing the numbering scheme.

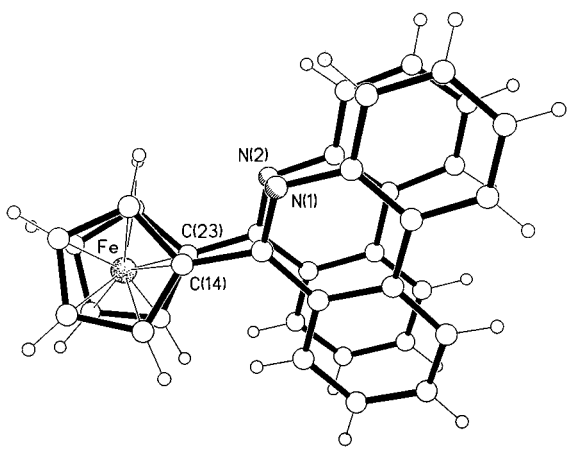

Fig. 2. Molecular structure of 1 highlighting the eclipsed geometry.

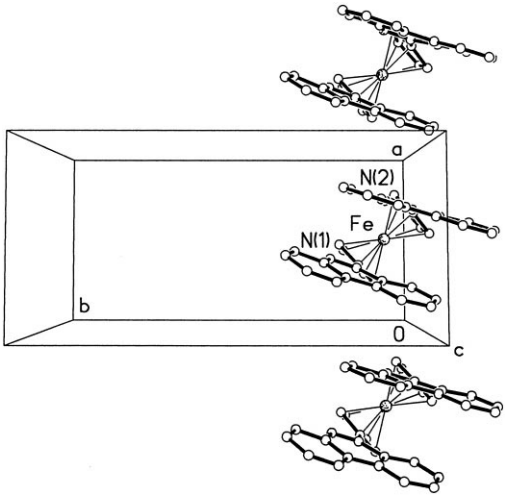

Fig. 3. Crystal packing in **1** illustrating the stacking of the phenanthridine moieties along the *a*-axis.

tal packing is such that the phenanthridine ligands are stacked along the *a*-axis (Fig. 3).

2.3. Attempted alkylation reactions

In an effort to confer water solubility on **1**, attempts to alkylate the phenanthridine nitrogen atoms with iodomethane were undertaken, but these were not successful. As a means of assessing the steric demands of such substitutions the molecular structure of **1** was used as a basis for simple modelling. Methyl groups were attached to the two nitrogen atoms with bond lengths of 1.5 Å, the typical value observed for ethidium bromide [14]. Fig. 4 shows orientations of the model of the alkylated derivative of **1** with the ferrocenyl group in the least sterically demanding *transoid* conformation. Each phenanthridinium ring is oriented differently in order to demonstrate the geometric effects. In the model, the right-hand phenanthridinium ring is in the conformation observed in the solid state and here the least sterically demanding conformation for the methyl group, found by rotation around the H_3C–N bond, produces $H_{Me}\cdots H_{Cp}$ distances of 1.53 Å ($H_c\cdots H_d$ and $H_c\cdots H_e$ on Fig. 4). The left-hand phenanthridinium moiety is rotated around the C_{Phen}–C_{Cp} bond so as to minimise steric interactions between the methyl group and the ferrocenyl moiety. The resulting torsion angle C_{Cp}–C_{Cp}–C_{Phen}–N is 85°, which brings $H_{Phen}\cdots H_{Cp}$ into contact with a separation of 0.95 Å ($H_a\cdots H_b$ in Fig. 4). Comparison with ethidium bromide also reveals a torsion angle between the phenyl and phenanthridinium groups of 85° (angle C_{Ph}–C_{Ph}–C_{Phen}–N) [14]. However, here for the analogous interactions the distances between the alkyl and phenyl H-atoms $H_{CH}\cdots H_{Ph\text{-}ortho}$ are 2.659 and 3.528 Å [14]. Hence, it is suggested that the steric demands of the ferrocenyl group preclude alkylation of the phenanthridine moieties.

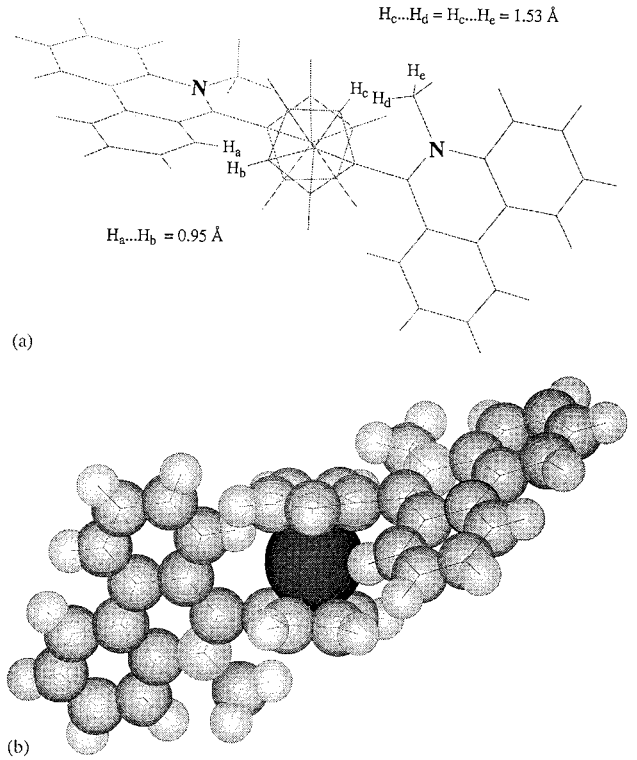

Fig. 4. Molecular model of 1,1′-bis(5-phenanthridium)ferrocene: (a) view along the Cp–Fe–Cp axis indicating the close approach of the H···H contacts; (b) space-filling representation.

2.4. Cyclometallation of 2-ferrocenyl-1,10-phenanthroline

Butler has previously reported the formation of the coordination compounds [$PdCl_2$(2-ferrocenyl-1,10-phenanthroline)] and [PdCl(6-ferrocenyl-2,2′-bipyridyl)] from reactions of the appropriate ferrocenyl-heterocycle with (1,5-cyclooctadienyl)palladium dichloride in CH_2Cl_2 [2]. The former involves coordination of the nitrogen donor atoms of the heterocycle only, while the latter features additional coordination with the formation of a metal–carbon bond through cyclometallation of the Cp ring.

We were interested in the formation of compounds analogous to [PdCl(2-phenyl-1,10-phenanthroline)] and its derivatives due to their reported interactions with nucleic acids [8,9]. Studies of the interactions of these complexes with DNA revealed two modes of binding, an intercalative mode and a covalent mode, with derivatives displaying some selectivity in binding to dG residues in DNA. Moreover, in the presence of H_2O_2 the methoxy derivative generated nicks at dG, and to a lesser extent, dA sites along the DNA [8].

Reaction of an aqueous solution of K_2PdCl_4 and a methanolic solution of 2-ferrocenyl-1,10-phenanthroline yielded after 3 days a purple solid. ^{1}H-NMR indicated the formation of a cyclometallated product with the appearance of three resonances for the substituted Cp

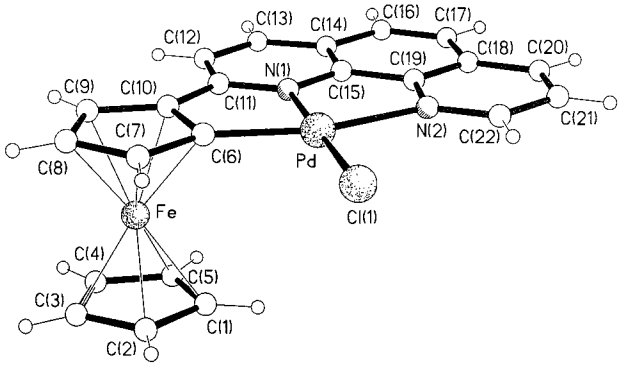

Fig. 5. Molecular structure of [Pd{(η^5-C_5H_5)Fe(η^5-C_5H_3(phenantholine))}Cl] (**2**), showing the numbering scheme.

ring each integrating to one proton. The effect of metallation upon the chemical shifts is not large, with the resonances for the three unique protons of the Cp ring lying within the chemical shift range of α and β protons of the starting material (4.62, 4.68, 5.01 vs. 4.35 (β) and 5.10 (α) ppm). This is similar to the case with ferrocenyl-2,2′-bipyridine where cyclopalladation has relatively little effect on the chemical shifts of the Cp protons (4.58, 4.66 and 4.93 versus 4.40 (β) and 5.01 (α) ppm) [2]. Confirmation of the nature of the product was obtained by single-crystal X-ray analysis.

2.5. Crystal structure of [Pd{($\eta^5C_5H_5$)Fe($\eta^5C_5H_3(C_{12}H_7N_2)$)}Cl] (**2**·0.5$CH_2Cl_2$)

Crystals suitable for X-ray crystallography were prepared by slow evaporation from a solution in dichloromethane. The molecular structure including the atomic numbering scheme is shown in Fig. 5, with selected bond lengths and angles presented in Table 2. The Cp rings of the ferrocene are effectively eclipsed (1.2°) with an interplanar angle of 3.7°. The iron-ring centroid distances are 1.655 Å to the unsubstituted Cp and 1.639 Å to the substituted Cp. The range of Fe–C distances is 2.031(3)–2.061(3) Å (mean 2.044 Å) with the longest Fe–C distance being to the cyclometallated carbon atom, C(6). The C–C bond lengths of the Cp rings lie in the range 1.404(6)–1.455(6) Å, with the longest bond length associated with the chelate ring, C(10)–C(6). These observations are mirrored by reported structures in which ferrocenyl moieties are involved in cyclometallated Pd complexes [4,15].

The metallocyclic ring is essentially coplanar to the substituted Cp ring (dihedral angle 1.7°), with the Pd metal centre adopting a distorted square-planar geometry with N(1) and N(2) of the phenanthroline ligand, C(6) of the substituted Cp ring, and Cl(1). These compare well with those from the disubstituted 2,2′-bipyridyl derivative reported by Butler [2]; Pd(1)–N(1), 1.998(15); Pd(1)–N(2), 2.158(16); Pd(1)–C(22), 1.926(17); Pd(1)–Cl(1), 2.307(5)Å. The Pd–C bond length in **2** also compares favourably with other cyclopalladated ferrocene derivatives, for example a value of 1.968 Å is seen in [PdClL(*N*,*N*′-dimethylaminomethylferrocene)] (where L = 1-methylimidazol-3-yl) [4]. The bond lengths associated with the phenanthroline show little deviation from those of the free ligand [16].

Table 2
Selected bond lengths (Å) and angles (°) for [Pd{($\eta^5C_5H_5$)Fe($\eta^5C_5H_3(C_{12}H_7N_2)$)}Cl], **2** · 0.5$CH_2Cl_2$

Bond lengths			
Pd–N(1)	1.976(3)	C(10)–C(9)	1.427(4)
Pd–N(2)	2.168(3)	C(9)–C(8)	1.419(5)
Pd–C(6)	1.974(3)	C(8)–C(7)	1.432(5)
Pd–Cl(1)	2.3130(9)	C(7)–C(6)	1.423(4)
C(11)–C(10)	1.456(4)	C(6)–C(10)	1.455(5)
C(11)–N(1)	1.340(4)	C(1)–C(2)	1.416(6)
N(1)–C(15)	1.354(4)	C(2)–C(3)	1.417(6)
C(15)–C(19)	1.426(4)	C(3)–C(4)	1.404(6)
Fe–Cp_{Sub} [a]	1.639	C(5)–C(1)	1.413(6)
Fe–Cp_{Unsub} [a]	1.655		
Bond angles			
Cl(1)–Pd–N(2)	100.42(8)		
N(2)–Pd–N(1)	79.43(10)		
N(1)–Pd–C(6)	80.60(12)		
C(6)–Pd–Cl(1)	99.54(10)		

[a] Cp represents the ring centroid.

Of further interest are the modes of molecular packing present in the crystal lattice, in which two factors are noteworthy. First, the unsubstituted Cp of one molecule C(1)–C(5) interacts through π–π stacking with the central six-membered ring (C(14)′–C(19)′) of the phenanthroline ligand of an inversion-related molecule (Fig. 6). The mean interplanar separation between the Cp and the phenanthroline is ca. 3.4 Å. Additionally, more complex π–π stacking interactions

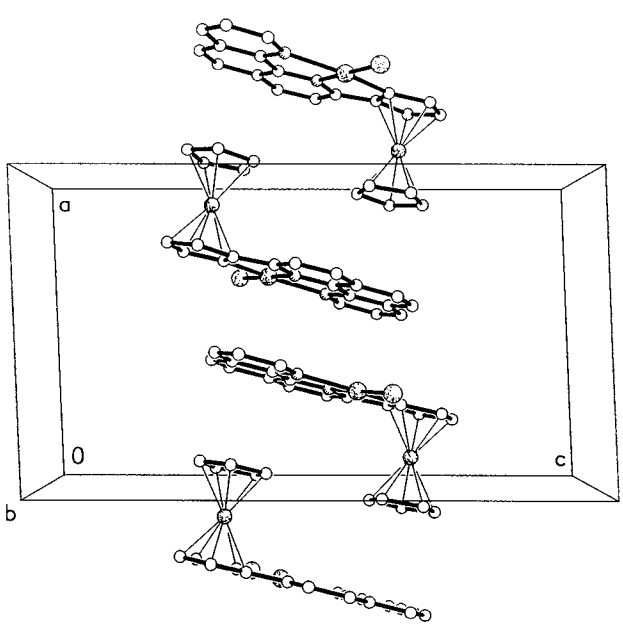

Fig. 6. Molecular packing present in the crystal lattice of **2**.

Table 3
Formal electrode potentials (vs. $Fc^+ \mid Fc$) for the one-electron oxidation of some ferrocenyl complexes [a]

Complex	$E^0(Fc^+ \mid Fc)$, V (vs. $Fc^+ \mid Fc$)
2-Ferrocenyl-1,10-phenanthroline [b]	+0.056
1,1′-bis(5-Phenanthridine)ferrocene (**1**) [c]	+0.075
[Pd{($\eta^5C_5H_5$)Fe($\eta^5C_5H_3$($C_{12}H_7N_2$))}Cl] (**2**) [b]	−0.031

[a] The electrolyte was $[N(Bu^t)_4,PF_6]$ in acetonitrile in each case, using a 1 mm diameter gold working electrode, a tungsten counter electrode and a silver wire as a quasi-reference electrode.
[b] Cyclic voltammetry, scan rate 0.1 V s^{-1}.
[c] Differential pulse voltammetry, scan rate 0.02 V s^{-1}.

occur between the {Cp_{Sub}/phenanthroline/Pd} groups of inversion-centre-related molecules, also with an interplanar separation of ca. 3.4 Å. These interactions produce stacks of molecules along the *a*-axis.

2.6. Electrochemistry

The formal electrode potentials (vs. $Fc^+ \mid Fc$) for the complexes 2-ferrocenyl-1,10-phenanthroline, 1,1′-bis(5-phenanthridine)ferrocene and [Pd{($\eta^5C_5H_5$)Fe($\eta^5C_5H_3$-($C_{12}H_7N_2$))}Cl] are presented in Table 3. A cyclic voltammogram of 2-ferrocenyl-1,10-phenanthroline reveals a reversible one-electron wave with a formal potential, E^0, of + 0.056 V (vs. $Fc^+ \mid Fc$). The positive shift in the electrode potential indicates more difficulty in the oxidation of the ferrocenyl unit compared with ferrocene, which is consistent with the expected electron-withdrawing effect on the cyclopentadienyl ring of the phenanthroline substituent. An even greater positive shift is exhibited for 1,1′-bis(5-phenanthridine)ferrocene due to the presence of two electron-withdrawing substituent groups, and indeed this is the case; with E^0 + 0.075 V (vs. $Fc^+ \mid Fc$), this again shows a reversible one-electron wave.

A cyclic voltammogram of the cyclopalladated derivative **2** reveals the presence of a ferrocenyl-based reversible one-electron oxidation, E^0 − 0.031 V. Cyclopalladation of 2-ferrocenyl-1,10-phenanthroline appears to facilitate the oxidation of the iron centre, E^0 − 0.031 cf. + 0.056 V. This is in agreement with previously reported results on the effects of cyclopalladation upon N-donor ferrocenyl ligands [4]. The greater electron density allowing for the easier oxidation of the Fe(II) centre in **2** must presumably arise through the Pd–$C_{(ferrocene)}$ bond as no significant reduction in the electron-withdrawing ability of the phenanthroline ligand would be expected upon coordination of the N donor atoms to Pd.

3. Experimental

^{1}H-NMR spectra were measured at 500.16 MHz on a Joel Lambda 500 NMR spectrometer. Mass spectrometry was carried out at the EPSRC National Mass Spectrometry Service Centre, The University of Wales, Swansea. X-ray crystallographic data were collected on a Bruker AXS SMART CCD area-detector diffractometer. All chemicals were purchased from Aldrich unless otherwise stated. Ether was dried by distillation over sodium wire under N_2. Electrochemical measurements were carried out in a conventional two-compartment glass cell using a EG&G model 263A potentiostat.

3.1. Preparation of 1,1′-bis(5-phenanthridine)ferrocene

Ferrocene (2.0 g, 10.8 mmol) was placed in a flame-dried Schlenk flask. The flask was evacuated and refilled with nitrogen, before the addition of 30 ml of dry diethyl ether. To this a solution of *n*-butyllithium (1.6 M in hexanes, 8.0 ml, 12.8 mmol) was added, followed by dry tetramethylethylenediamine (1.2 g, 30.0 mmol). The solution was left to stir overnight, by which time a pale orange precipitate of lithiated ferrocene had formed. The solution was cooled to − 70°C (acetone–dry ice), followed by the addition of a 10% molar excess of phenanthridine (2.5 g, 14.1 mmol). After allowing the reaction mixture to warm up slowly to 18°C, it was stirred for 3 days before being hydrolysed under aerobic conditions with water. The organic layer was separated and the remaining solid was further extracted with dichloromethane. The combined organic fractions were taken to dryness, to leave brown oil. Column chromatography on silica using hexanes–ether (5:5) afforded a major product identified as 1,1′-bis(5-phenanthridine)-ferrocene in relatively low yield (10%). A very low yield of a second product was obtained (3%) which, based on ^{1}H-NMR, was identified as the mono-substituted derivative 6-ferrocenyl-5-phenanthridine.

3.1.1. 6-Ferrocenyl-5-phenanthridine

^{1}H-NMR, (500 MHz, $CDCl_3$) δ 4.1 (s, 5H, C_5H_5), 4.4 (t, 2H, β protons from C_5H_4), 5.0 (t, 2H, α protons from C_5H_4), 7.5–9.5 (8H, protons from $C_{13}H_8N$). Yield: 2%. MS: m/z 363 [M^+]. Elemental analysis for $C_{23}H_{17}NFe$. Found (Anal. Calc.) C, 75.97 (76.05); H, 4.41 (4.71); N, 3.85 (3.66).

3.1.2. 1,1′-Bis(5-phenanthridine)ferrocene

^{1}H-NMR, (500 MHz, d_6DMSO) δ 4.6 (s, 4H, β protons from 2 × C_5H_4), 5.15 (s, 4H, α protons from 2 × C_5H_4), 7.0–9.0 (16H, protons from 2 × $C_{13}H_8N$). Yield: 10%. MS: m/z 540 [M^+]. Elemental analysis for $C_{36}H_{24}N_2Fe$. Found (Anal. Calc.) C, 80.07 (80.00); H, 4.13 (4.47); N, 5.26 (5.18).

3.2. Preparation of [Pd{($\eta^5C_5H_5$)Fe($\eta^5C_5H_3$($C_{12}H_7N_2$))}Cl]

To potassium tetrachloropalladate (0.07 g, 0.22 mmol) in the minimum amount of water, was added a

Table 4
Crystallogrphic data

Compound	**1**	**2**
Empirical formula	$C_{36}H_{24}FeN_2$	$C_{22}H_{15}ClFeN_2$-Pd·0.5CH_2Cl_2
M	540.4	547.5
Crystal system	Monoclinic	Monoclinic
Space group	$P2_1/n$	$P2_1/c$
Unit cell dimensions		
a (Å)	7.4642(6)	10.6066(7)
b (Å)	15.2523(12)	9.5702(7)
c (Å)	21.1851(17)	18.7806(13)
β (°)	96.582(2)	92.144(2)
V (Å^3)	2395.9(3)	1905.0(2)
Z	4	4
D_{calc} (g cm^{-3})	1.498	1.909
μ (mm^{-1})	0.66	2.00
T (K)	160	160
Crystal size (mm)	$0.90 \times 0.80 \times 0.02$	$0.26 \times 0.13 \times 0.11$
θ_{max} (°)	28.3	28.7
Maximum indices hkl	9,20,28	13,12,25
Transmission factor range	0.762–0.928	0.658–0.802
Reflections measured	16810	12046
Unique reflections	5438	4560
R_{int}	0.0292	0.0267
Number of parameters	352	262
$R(F)$ ('observed data')	0.0334	0.0385
R_w (F^2) (all data)	0.0832	0.0796
Goodness-of-fit	1.010	1.117
Max, min el. density (e Å^{-3})	0.321, −0.406	1.194, −0.992

solution of 2-ferrocenyl-1,10-phenanthroline [2] (0.08 g, 0.22 mmol) in the minimum amount of methanol. Immediately upon mixing a purple precipitate appeared. The solution was allowed to stir for 3 days. Filtration yielded a purple solid, which was washed with methanol and allowed to dry. Crystals suitable for X-ray crystallography were prepared by slow evaporation from a solution in dichloromethane.

^{1}H-NMR, (500 MHz, d_6DMSO) δ 4.11 (5H, s, C_5H_5), 4.62 (1H, s, proton from C_5H_3), 4.68 (1H, s, proton from C_5H_3), 5.01 (1H, s, proton from C_5H_3), 8.0 (1H, d,), 8.15 (3H, m), 8.7 (1H, d), 8.85 (1H, d), 8.95 (1H, d)-protons of phenanthroline. Yield: 89%. MS: m/z 506 [M$^+$]. Elemental analysis. Found (Anal. Calc.) for $C_{22}H_{15}ClFeN_2Pd{\cdot}CH_2Cl_2$: C, 46.40 (46.82); H, 2.76 (2.90); N, 4.55 (4.75).

3.3. X-ray crystallography

Crystallographic data for **1** and **2**$\cdot 0.5CH_2Cl_2$ are in Table 4. Data were collected on a Bruker AXS SMART CCD diffractometer with Mo–K_α radiation ($\lambda = 0.71073$). Semi-empirical absorption corrections were applied, based on symmetry-equivalent and redundant data.

The structures were solved by automatic direct methods and refined on F^2 values for all unique data, with anisotropic displacement parameters and with a riding model for isotropic H atoms. Solvent CH_2Cl_2 is disordered over an inversion centre in the crystal structure of **2**·0.5CH_2Cl_2, and the largest difference map features are in this region, for which structural modelling is imperfect.

Programs were standard Bruker AXS control and integration software and SHELXTL (G.M. Sheldrick), together with local programs. Crystallographic data for the structural analysis have been deposited with the Cambridge Crystallographic Data Centre, 12 Union Road, Cambridge CB2 1EZ, UK, CCDC nos. 132709 and 132710 for compounds **1** and **2**, respectively.

Acknowledgements

The EPSRC are thanked for a studentship (C.J.I.) and for equipment funding.

References

[1] I.R. Butler, J.L. Roustan, Can. J. Chem. 68 (1990) 2212.
[2] I.R. Butler, Organometallics 11 (1992) 74.
[3] P.D. Beer, J.P. Danks, M.G.B. Drew, J.F. McAleer, J. Organomet. Chem. 476 (1994) 63.
[4] C. Lopez, R. Bosque, X. Solans, M. Font-Bardia, D. Tramuns, G. Fern, J. Silver, J. Chem. Soc. Dalton Trans. (1994) 3039.
[5] S. Takenada, Y. Uto, H. Saita, M. Yokoyama, H. Kondo, D. W. Wilson, Chem. Commun. (Cambridge) (1998) 111.
[6] C.-W. Ong, J.-Y. Jeng, S.-S. Juang, C.-F. Chen, Bioorg. Med. Chem. Lett. 2 (1992) 929.
[7] H. Tamura, M. Miwa, Chem. Lett. (1997) 1177.
[8] (a) R.G. Newkome, M. Onishi, W.E. Puckett, W.A. Deutsch, J. Am. Chem. Soc. 102 (1980) 4551. (b) T.D. Tullis (Ed.), Metal-DNA Interactions, ASC, Washington DC, 1989, Chapter 10. (c) J.W. Suggs, J.D. Higgins, R.W. Wagner, J.T. Millard, ACS Symp. Ser. 402 (1989) 146.
[9] J.W. Suggs, M.J. Dube, N. Nichols, J. Chem. Soc. Chem. Comm. (1993) 307.
[10] R.A. Abramovitch, C.S. Gaim, Can. J. Chem. 42 (1964) 1627.
[11] I.R. Butler, L.J. Hobson, S.J. Coles, M.B. Hursthouse, K.M. Abdul-Malik, J. Organomet. Chem. 27 (1997) 540.
[12] F.H. Allen, O. Kennard, Chem. Design Autom. News 8 (1993) 31.
[13] P. Roychowdbury, Acta. Crystallogr. Sect. B 29 (1973) 1362.
[14] E. Subramanian, J. Trotter, C.E. Bugg, J. Cryst. Mol. Struct. 1 (1971) 3.
[15] P.R.R. Ranatunge-Banarage, B.H. Robinson, J. Simpson, Organometallics 13 (1994) 500.
[16] L.A. Summers, Adv. Heterocycl. Chem. 22 (1978) 2.